J Math Chem (2018) 56:2496–2511
https://doi.org/10.1007/s10910-018-0901-x

ORIGINAL PAPER

Skeletal and reduced chemical mechanism for hydrogen fluoride chemical laser

Hui Li[1,2] · Shuqin Jia[1] · Tianliang Zhao[1] · Ying Huai[1]

Received: 10 September 2017 / Accepted: 22 March 2018 / Published online: 9 April 2018

Abstract The chemical kinetics of supersonic hydrogen fluoride (HF) chemical lasers determines combustion characteristics and output power. However, the inherent complexity of chemical reactions and complex structure still challenge the numerical simulations involving a comprehensive chemical mechanism. Therefore, a high fidelity and low computational consuming model is important for design purpose. This paper presents a strategy to generate a reduced mechanism for HF chemical lasers. Based on a detailed HF chemical mechanism consisting of 16 species and 153 elementary reactions, a specific skeletal mechanism including 11 species and 58 elementary reactions is generated. Finally, we obtain a further reduction mechanism including 11 species and 39 elementary reactions by combining sensitivity analysis and rate of production analysis. The computational cost for simulation of supersonic HF chemical lasers with the reduced mechanism is less than that with the detailed model. The principal contribution of the work is to provide a low computational consuming model.

Keywords Chemical laser · SA · DRG · Reduced mechanism · Rate of production

1 Introduction

In the middle 1960s, HF chemical lasers have been extensively studied and the pumping reactions are the paradigm for exothermic triatomic chemical reactions [1]. Despite enormous experiments and theoretical research expended to make a better under-

✉ Ying Huai
huaiying@dicp.ac.cn

1 Key Laboratory of Chemical Lasers, Dalian Institute of Chemical Physics, Chinese Academy of Sciences, Dalian 116023, China

2 University of Chinese Academy of Sciences, Beijing 100049, China

standing on the performance of supersonic HF chemical lasers. However, the inherent complexity of the HF chemical reactions and complex structure of the supersonic flow still be a big challenge to of numerical simulations of continuous wave HF chemical lasers devices. In the frame of computational flow dynamics, the influence of chemical reactions on the flow processes is by loading chemical reactions sources term in the species transport equations. As we all know, the kinetic models have strongly impact on the numerical results. Meanwhile, numerical simulations involving a detailed state-to-state chemical mechanism are prohibitive for real large-scale HF chemical lasers. Consequently, a highly fidelity and less time-consuming model is necessary to simulate HF chemical lasers.

High-intensity 2.7 μm fundamental HF laser relies on exothermic chemical or energy transfer reactions to produce population inversion in the product species. The pumping reactions are given:

$$F + H_2 \rightarrow HF + H, \tag{R1}$$

$$H + F_2 \rightarrow HF + F. \tag{R2}$$

These two reactions can generate partial inversion between several ro-vibrational levels in different vibrational states and the excited states of HF (υ, J) are rapidly quenched by collisions with corresponding species. Emanuel present a theory for HF chemical laser under continuous wave conditions and analyzed the influence of parameters of the system [2]. The kinetic packages of the HF chemical lasers has been published in 1976–1977 [3] and in 1982 [4]. The state-to-state kinetic model has been widespread in numerical simulation. Numerical results of non-premixed supersonic combustion with different fuel/oxidant has been obtain insight into the mechanism of coupling between the process in the combustion region and in the supersonic supply system with 13 species and 165 elementary reactions [5, 6]. In fact, most of these researches has focus on large-scale laser technology demonstrations. However, the development of chemical mechanism of HF lasers is very slowly. In 2002, Manke II and Hager published a new review based on the analysis of experimental and theoretical data and recommended corresponding rate constants [7]. This package has been used until now, and in this package, many rate constants has no change, but exception of multi-quantum collisional HF (υ) deactivation by HF, DF, F has been confirmed. Comparison of these well-known kinetic models by analyzing the small single gain, which the difference reaches 40–60%, by simply adding and subtracting elementary reactions [8]. In fact, HF lasers are strongly coupled with rapid and effective mixing of the reagent gas, it is not yet draw accurate, unambiguous conclusions about the package [9]. In current works, we attempt to provide a less time consuming mechanism for design purpose and make a further understanding on chemical mechanism.

Many scholars have proposed different methodologies for mechanisms reduction. There are two major categories of reduction techniques for reduction mechanisms, namely species-based elimination and time-scale analysis. The first strategy is to generate a skeletal mechanism by eliminating redundant species and corresponding elementary reactions. In species eliminating methods, DRG method has been proved to be an efficient tool to construct skeletal mechanism, introduced by Lu and Low

[10]. Subsequently, some methods based on the DRG method have been put forward to improve and modify the results of reduction, such as the DRG with error propagation (DRGEP) [11]. The second strategy is time-scale analysis. Time-scale analysis is based on the observation that there are frequently highly reactive radicals or fast reactions in detailed chemistry, resulting in vastly different time scales and stiffness in the system [12]. These methods are based the assumption that the system is quasi-steady-state and partial equilibrium reactions. Such as the computational singular perturbations (CSP) [13, 14], quasi-steady-state approximation (QSSA) [15].

The primary purpose of this paper is to develop a fidelity and less time-consuming model using DRG and Sensitivity Analysis methods, based on a detail mechanism including 16 species and 153 reactions. Results of small single gain has been obtained to validate the less time-consuming model with two-dimensional computational fluid dynamics.

2 Reduction methodologies

Sensitivity analysis can be used to understand the relationship between the values of the input parameters of a mathematical model and its solutions. The data source of the sensitivity analysis can help to gain a better understanding of the chemical processes and identify the key model output or production distributions. For a spatially homogeneous system, the change of the variable $\boldsymbol{Y}$ in time is calculated from the following ordinary differential equation (ODE):

$$\frac{d\,\mathbf{Y}_i}{dt} = f(\mathbf{Y}, \mathbf{x}). \tag{1}$$

The effect of changes in parameter set $\mathbf{x}$ on the concentrations at a given time can be characterized by the following Taylor expansion:

$$Y_i(t, x + \Delta x) = Y_i(t, x) + \sum_{j=1}^{m} \frac{\partial Y_i}{\partial x_i} \Delta x_i \; + \frac{1}{2} \sum_{k=1}^{m} \sum_{j=1}^{m} \frac{\partial^2 Y_i}{\partial x_k \partial x_i} \Delta x_k \Delta x_j \; + \cdots . \tag{2}$$

In Eq. (5), $\partial Y_i/\partial x_j$ is the first-order local sensitivity coefficient; $\partial^2 Y_i/\partial x_j \partial x_k$ is the second-order local sensitivity coefficient. The normalized sensitivity coefficient matrix $\boldsymbol{S} = (x_j/Y_i)(\partial Y_i/\partial x_j)$ is to take account of the different units between input parameters and outputs such as concentrations or temperature [16]. For reactions rate sensitivity, the variant x_i represent the pre-exponential "A-factors" in the Arrhenius reaction rate expressions. In the present work, the sensitivity coefficient matrix is calculated by using the homogeneous batch reactor model with SENKIN code [17].

Direct Relation Graph method introduced by Lu and Law [10] makes an important contribution to generate skeletal mechanisms with the merit in clear concept and less computation time consuming. However, it is far more complicated to identify and to remove the redundant species because of the strongly coupled species. In the DRG method, the direct interaction coefficient between the two-coupled species is defined as:

$$r_{AB}^{DRG} = \frac{\sum_{i=1,I} \left| v_{A,i}\omega_i \delta_B^i \right|}{\sum_{i=1,I} \left| v_{A,i}\omega_i \right|}, \tag{3}$$

$$\delta_B^i = \begin{cases} 1, & \text{if the } i \text{ th reaction involves species B} \\ 0, & \text{otherwise} \end{cases}, \tag{4}$$

where r_{AB} ($0 < r_{AB} < 1$) is the interaction coefficient of the species A and species B, respectively. $v_{A,i}$ is the net stoichiometric coefficient of species A, ω_i is the net reaction rate of the ith reaction. In order to quantify the relationship between species, we define a threshold ε to generate a skeletal mechanism with different levels of accuracy. In the DRG method, each species is assumed to be equally important and only direct relation between two species is calculated.

Pepiot-Desjardins has proposed a directed relation graph with error propagation method (DRGEP), where coupling between two species through all possible pathway is considered [11]. The following interaction coefficient r_{AB} is written explicitly as:

$$r_{AB} = \frac{\sum_{i=1,I} \left| v_{A,i}\omega_i \delta_B^i \right|}{\max(P_A, C_A)}, \tag{5}$$

$$P_A = \sum_{i=1,I} \max(0, \upsilon_{Ai}\, \omega_i), \tag{6}$$

$$C_A = \sum_{i=1,I} \max(0, -\upsilon_{Ai}\, \omega_i), \tag{7}$$

where P_A and C_A are the production and consumption rate of species A. After calculating the direct interaction coefficient for all species pairs, a path dependent interaction coefficient $r_{AB,P}$ is calculated through a damping procedure,

$$r_{AB,p} = \prod_{i=1}^{n-1} r_{S_i S_{i+1}}. \tag{8}$$

In Eq. (11), S is the generic intermediate species, interposing in the pth reactions path between the species A and B. In the DRGEP methods, if species A is kept in the mechanism, all other species that are reachable for species A though direct and indirect coupling are calculated using the overall interaction coefficient. The interaction coefficient is described as:

$$R_{AB} = \max_S \left(r_{AB,p} \right). \tag{9}$$

The DRGEP method then performs an efficient breadth-first search algorithm [18]. For a given error limit, an iterative search algorithm chose the optimal threshold ε by taking the following steps. First, starting with a low value of 0.001, the algorithm generates an initial skeletal mechanism and calculates the maximum error of the corresponding parameter for all initial conditions using,

$$E_i = \max_j \frac{\left|\delta_{i,j} - \delta_{\text{detail},j}\right|}{\delta_{\text{detail},j}}, \tag{10}$$

where δ is the concentration of species or other parameter from the skeletal mechanism through removal of the *i*th species in the indeterminate set at the condition. The small E_i of the species will be eliminated from the mechanism, and then a skeletal mechanism is generated with the specified error limit.

Following removal of a large number of species by the DRG and DRGEP method, a sensitivity analysis is performed in the following steps: (1) when the skeletal mechanism is generated. (2) Remove each candidate species individually from the smallest acceptable skeletal mechanism generated by DERGEP and calculate the induced error on target parameters for the target species. (3) Rank the candidate species by using their induced error in ascending order. (4) Remove candidate species from the smallest skeletal mechanism generated by DRGEP in order as prescribed in step 3 and calculate the cumulative induced error and target-induced error on target parameters after each species is removed. Stop the process when the cumulative induced error is beyond the tolerance level.

3 Chemical reaction model

In continuous-wave HF chemical laser system, the oxidant F and the fuels H_2 and dilute gas are expanding through supersonic multi-nozzle bank into the cavity in a very short time. In addition, the chemical kinetics requires flow at very high velocity and low pressure which results in low Reynolds number or laminar flow with extended mixing lengths. In order to identify the main features of chemical mechanism in the cavity, we adopt Perfectly Stirred Reactor (PSR) model to develop a reduced mechanism with some certain assumptions.

One of the key parameters determining the laser power and which could be measured experimentally is the small signal gain (SSG). It's always used to validate the numerical simulation results. The small singal gain of the medium is a function of population of the upper and lower quantum energy states

$$\gamma(\upsilon) = \sigma(\upsilon)\left[N_u - \frac{g_u}{g_l}N_l\right], \tag{11}$$

where N_u and N_l are the upper and lower energy states number densities, respectively. g_u and g_l are the degeneracies of the upper and lower energy level, respectively, and the σ(υ) is the stimulated emission cross section given by

$$\sigma_{\text{stim}}(\upsilon) = \frac{c^2 A_{\text{um}}}{8\pi\upsilon^2} f(\upsilon), \tag{12}$$

where A_{nm} is the Einstein emission coefficient, υ is the transition frequency and the *f(υ)* is the spectroscopic line shape function.

Even though there are only 9 chemical species (F, F_2, HF, DF, H, H_2, H_2 (1), He, N_2), the chemistry of this system is extremely complex. In real system, the vibrational

levels is up to nine with up to 30 rotational levels, and each HF (υ, J) must be treated as individual species and be tracked [19].

This paper adopts the state-to-state kinetic model and the rate constants of dissociation–recombination, and the reactions of V–V and V–T energy exchange.

Pumping reaction:

$$\mathrm{F} + \mathrm{H_2} \rightarrow \mathrm{HF}\,(\upsilon) + \mathrm{H}, \tag{R1}$$

$$\mathrm{H} + \mathrm{F_2} \rightarrow \mathrm{HF}\,(\upsilon) + \mathrm{F}. \tag{R2}$$

Collisional relaxation:

$$\mathrm{HF}\,(\upsilon) + \mathrm{M} \rightarrow \mathrm{HF}\,(\upsilon - 1) + \mathrm{M} \tag{R3}$$

$$\mathrm{M} = \mathrm{HF},\ \mathrm{H_2},\ \mathrm{F},\ \mathrm{H},\ \mathrm{He},\ \mathrm{DF}$$

V–V energy transfer:

$$\mathrm{HF}\,(\upsilon) + \mathrm{HF}\,(\upsilon) = \mathrm{HF}\,(\upsilon - 1) + \mathrm{HF}\,(\upsilon + 1) \tag{R4}$$

$$\mathrm{HF}\,(\upsilon) + \mathrm{H_2}\,(0) = \mathrm{HF}\,(\upsilon) + \mathrm{H_2}\,(1) \tag{R5}$$

Dissociation reaction and recombination reaction:

$$\mathrm{F} + \mathrm{F} + \mathrm{M} = \mathrm{F_2} + \mathrm{M} \tag{R6}$$

$$\mathrm{H} + \mathrm{H} + \mathrm{M} = \mathrm{H_2} + \mathrm{M} \tag{R7}$$

$$\mathrm{F_2} + \mathrm{M} = 2\mathrm{F} + \mathrm{M} \tag{R8}$$

$$\mathrm{HF}\,(\upsilon) + \mathrm{M} = \mathrm{H} + \mathrm{F} + \mathrm{M} \tag{R9}$$

The rate constant are expression by modified Arrhenius equation

$$k_i = A_i T^b \exp\left(-\frac{E_a}{RT}\right), \tag{13}$$

where E_i is the energy of activation, A_i and b are the pre-exponential factor and temperature parameter, respectively. In addition, For such rate constant of the reactions: $k_0 = 6.0 \times 10^{11} T^{-1} + 1 \times 10^4 T^{2.28}$, the elementary reaction can be divided two individual duplicated reactions. Finally, a detailed mechanism contains 16 species and 153 elementary reactions has been constructed [1, 7].

4 The reduced mechanism for HF chemical lasers

The simulation are executed by using PSR model without heat loss. The initial temperature of 298 K, the range of the initial pressure is 3–10 Torr, and the initial mole fraction are listed in Table 1.

Table 1 The mole fraction at various equivalence ratios

Equivalence ratio	0.6			1.0			1.5		
Species	F	H_2	DF	F	H_2	DF	F	H_2	DF
Mole fraction	0.1854	0.1104	0.3574	0.1712	0.1784	0.1194	0.1616	0.2245	0.3115
Species	He	N_2	F_2	He	N_2	F_2	He	N_2	F_2
Mole fraction	0.2161	0.1293	0.0014	0.1997	0.1194	0.0013	0.1885	0.1127	0.0012

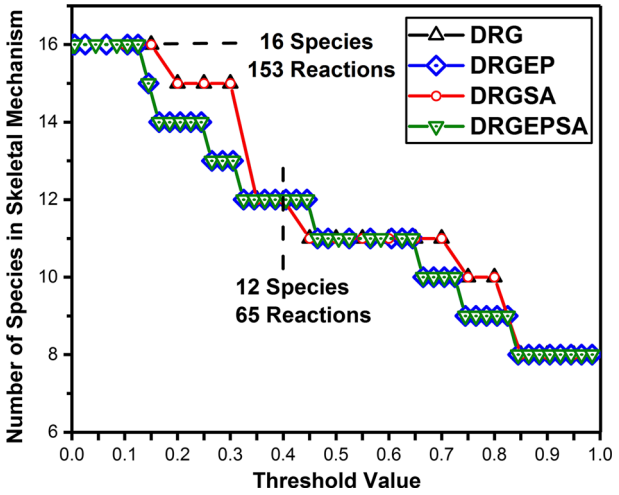

Fig. 1 Evolution of the species number of the skeletal mechanism on the threshold value ε. The results of DRG, and DRGSA coincide. The results of DRGEP and DRGEPSA coincide

In this paper, F, H_2 and temperature are selected as the starting conditions. Figure 1 shows the evolution of the number of species kept in skeletal mechanism versus the threshold values ε. Obviously, when the threshold ε is 0.01, the skeletal mechanism is almost the same to the detailed mechanism. And then when the threshold ε is 1.0, H, H_2, F, F_2, HF (1), DF, N_2 and He remain in the skeletal mechanism with 12 elementary reactions, which contains 10 third body reactions. It is obvious that the DRG and DRGSA methods almost generate the same skeletal mechanism along the threshold change. The strongly coupled species HF (4), HF (5), HF (6) come when threshold value ε is 0.3. However, the DRGEP and DRGEPSA methods show the sequence of removal species: HF (4), HF (7), HF (5), HF (6). When HF (3) is removed from the skeletal mechanism, target tolerance of the temperature has an apparent increase. In the HF chemical laser system, the calculation of small single gain relevant to HF (3) [8]. This paper analyzed that H_2 (1) almost has no influence on supersonic HF lasers. Unfortunately, the DRG, DRGEP and DRGEPSA cannot identify H_2 (1). Finally, a skeletal mechanism is generated including 11 species and 58 elementary reactions.

Because of various third body reactions retaining in the skeletal mechanism, a further reduction step is performed by using rate of production analysis and sensitivity analysis. Rate of production analysis provides complementary information on the direct contributions of individual reactions to species net production rates. The unimportant reactions can be eliminated from the skeletal mechanism if the contribution of *i*th reaction is less than the threshold value. In the current work, the threshold value is equal to 1.0E−11, the dissociation and recombination reactions of H_2, F_2, HF (υ) can be removed from the skeletal mechanisms. By combining rate of production analysis and sensitivity analysis, we developed a reduced mechanism containing 11 species and 39 reactions. Table 2 lists the reduced mechanism.

Figure 2 lists the sensitivity coefficients of the most important reactions for temperature. It is evident that these important elementary reactions in skeletal and reduced

Table 2 The reduced mechanism with 11 species 39 elemental reactions

No.	Reaction	No.	Reaction	No.	reaction
1	$F+H_2 => HF\ (1)+H$	14	$HF\ (3)+H => HF\ (1)+H$	27	$HF\ (1)+HF\ (2) => HF\ (0)+HF\ (3)$
2	$F+H_2 => HF\ (2)+H$	15	$HF\ (2)+H => HF\ (0)+H$	28	$HF\ (1)+N_2 => HF\ (0)+N_2$
3	$F+H_2 => HF\ (3)+H$	16	$HF\ (3)+H => HF\ (1)+H$	29	$HF\ (2)+N_2 => HF\ (1)+N_2$
4	$H+F_2 => F+HF\ (0)$	17	$HF\ (3)+H => HF\ (0)+H$	30	$HF\ (3)+N_2 => HF\ (2)+N_2$
5	$H+F_2 => F+HF\ (1)$	18	$HF\ (1)+F => HF\ (0)+F$	31	$HF\ (1)+N_2 => HF\ (0)+N_2$
6	$H+F_2 => F+HF\ (2)$	19	$HF\ (2)+F => HF\ (1)+F$	32	$HF\ (2)+N_2 => HF\ (1)+N_2$
7	$H+F_2 => F+HF\ (3)$	20	$HF\ (3)+F => HF\ (2)+F$	33	$HF\ (3)+N_2 => HF\ (2)+N_2$
8	$HF\ (3)+H=F+H_2$	21	$HF\ (1)+He => HF\ (0)+He$	34	$HF\ (1)+DF => HF\ (0)+DF$
9	$HF\ (1)+H_2 => HF\ (0)+H_2$	22	$HF\ (2)+He => HF\ (1)+He$	35	$HF\ (2)+DF => HF\ (1)+DF$
10	$HF\ (1)+H => HF\ (0)+H$	23	$HF\ (3)+He => HF\ (2)+He$	36	$HF\ (3)+DF => HF\ (2)+DF$
11	$HF\ (2)+H => HF\ (1)+H$	24	$HF\ (1)+HF\ (0) => 2HF\ (0)$	37	$HF\ (1)+DF => HF\ (0)+DF$
12	$2HF\ (1) => HF\ (2)+HF\ (0)$	25	$HF\ (2)+HF\ (0) => HF\ (1)+HF\ (0)$	38	$HF\ (2)+DF => HF\ (1)+DF$
13	$2HF\ (2) => HF\ (3)+HF\ (1)$	26	$HF\ (3)+HF\ (0) => HF\ (2)+HF\ (0)$	39	$HF\ (3)+DF => HF\ (2)+DF$

mechanism are almost the same as those in detailed mechanism and the values of sensitivity coefficient agree well with each elementary reaction. The results confirm that the dominant reactions are $F+H_2 => HF\ (2)+F$, $F+H_2 => HF\ (1)+F$, $H_2\ (1)+H=H_2+H$ and $F+H_2 => HF\ (3)+H$. As shown in Fig. 4, $F+H_2 => HF\ (2)+F$ and $F+H_2 => HF\ (1)+F$ have an positive influence on system temperature while the $H_2\ (1)+H=H_2+H$ and $F+H_2 => HF\ (3)+H$ have a negative influence on system temperature.

Figure 3 shows that the dominant reactions do not change as the equivalence ratio ϕ increased. Nevertheless, $H_2\ (1)+H=H_2+H$, $HF\ (3)+F => HF\ (2)+F$ and $F+H_2 => HF\ (3)+H$ have an significant fluctuation as ϕ increased. Furthermore, when $\phi > 1.0$, the gap of sensitivity coefficients between these reactions becomes smaller. It shows that the system temperature increases slower as equivalence ratio increases.

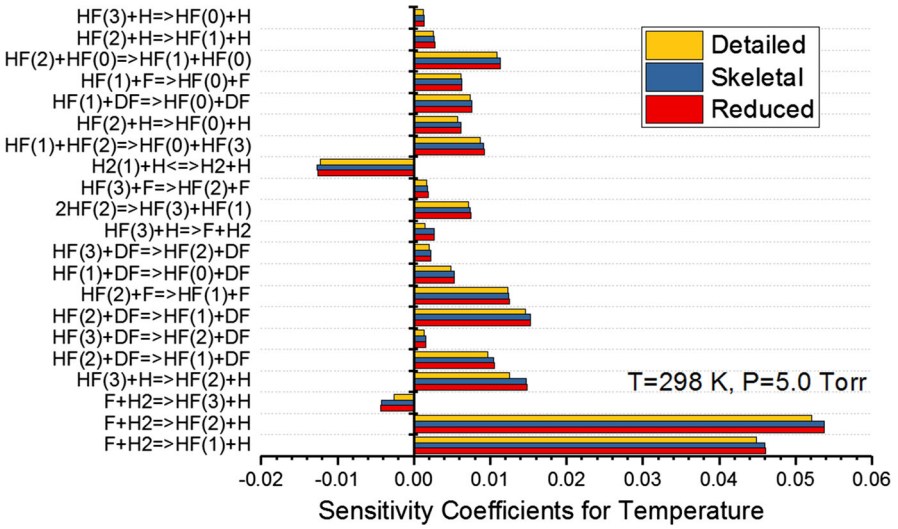

Fig. 2 Sensitivity coefficients for temperature of the most important reactions (T = 298 K, P = 5.0 Torr)

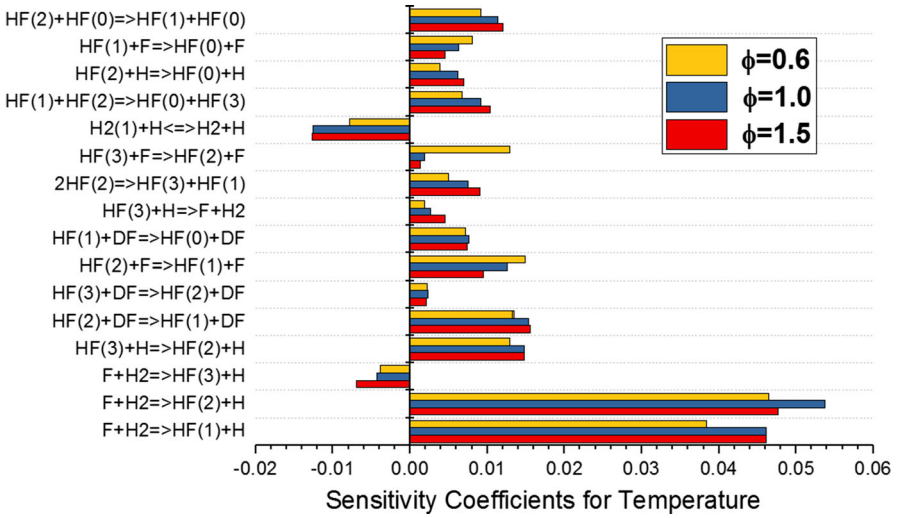

Fig. 3 Sensitivity coefficients for HF (2) over a range of equivalence ratio using the reduced mechanism

5 Numerical simulation of supersonic HF chemical lasers

The combustion driven HF overtone chemical lasers is composed of five parts: gas entering system, combustor, nozzle array, optical resonator and pressure recovery system. In order to validate the reduced mechanism, two-dimensional Navier–Stokes equations and species transport equation are applied to numerical analyze the mecha-

nism of optical resonator in supersonic HF chemical lasers. The conservation equations are in the following form:

$$\frac{\partial Q}{\partial t} + \frac{\partial E}{\partial x} + \frac{\partial F}{\partial y} = \frac{\partial E_v}{\partial x} + \frac{\partial F_v}{\partial y} + S_{\text{chem}}, \tag{14}$$

where Q is the conservative flow variable vector, and E and F are the inviscid flux vectors in the x, y directions, respectively. E_v and F_v are the viscous flux vectors. S_{chem} is the source vectors that indicate the rates of formation of chemical species due to the chemical reaction.

$$Q = \begin{pmatrix} \rho_1 \\ \rho u \\ \rho v \\ \rho e_t \\ \rho Y_i \end{pmatrix}, \quad E = \begin{bmatrix} \rho u \\ \rho u^2 + P \\ \rho uv \\ u(\rho e_t + P) \\ \rho u Y_i \end{bmatrix}, \quad F = \begin{bmatrix} \rho v \\ \rho uv \\ \rho v^2 + P \\ v(\rho e_t + P) \\ \rho v Y_i \end{bmatrix},$$

$$E_v = \begin{bmatrix} 0 \\ \tau_{xx} \\ \tau_{xy} \\ u\tau_{xx} + v\tau_{xy} - q_x + q_{sx} \\ d_x \end{bmatrix}, \quad F_v$$

$$= \begin{bmatrix} 0 \\ \tau_{xy} \\ \tau_{yy} \\ u\tau_{xy} + v\tau_{yy} - q_x + q_{xy} \\ d_y \end{bmatrix}, \quad S_{\text{chem}}$$

$$= \begin{bmatrix} 0 \\ 0 \\ 0 \\ 0 \\ \omega_i \end{bmatrix},$$

$$e_t = \sum_{i=1}^{NS} Y_i h_i - \frac{P}{\rho} + \frac{1}{2}\left(u^2 + v^2\right), \quad h_i = h_{fi}^0 + \int_{T_{ref}}^{T} C_{pi}\mathrm{d}T, \quad P = \rho R_u T \sum_{i=1}^{NS} \frac{Y_i}{W_i},$$

where e_t is the total internal energy, h is the enthalpy, C_{pi} is specific heat at constant pressure of ith species, P and T are the pressure and temperature of systems, respectively.

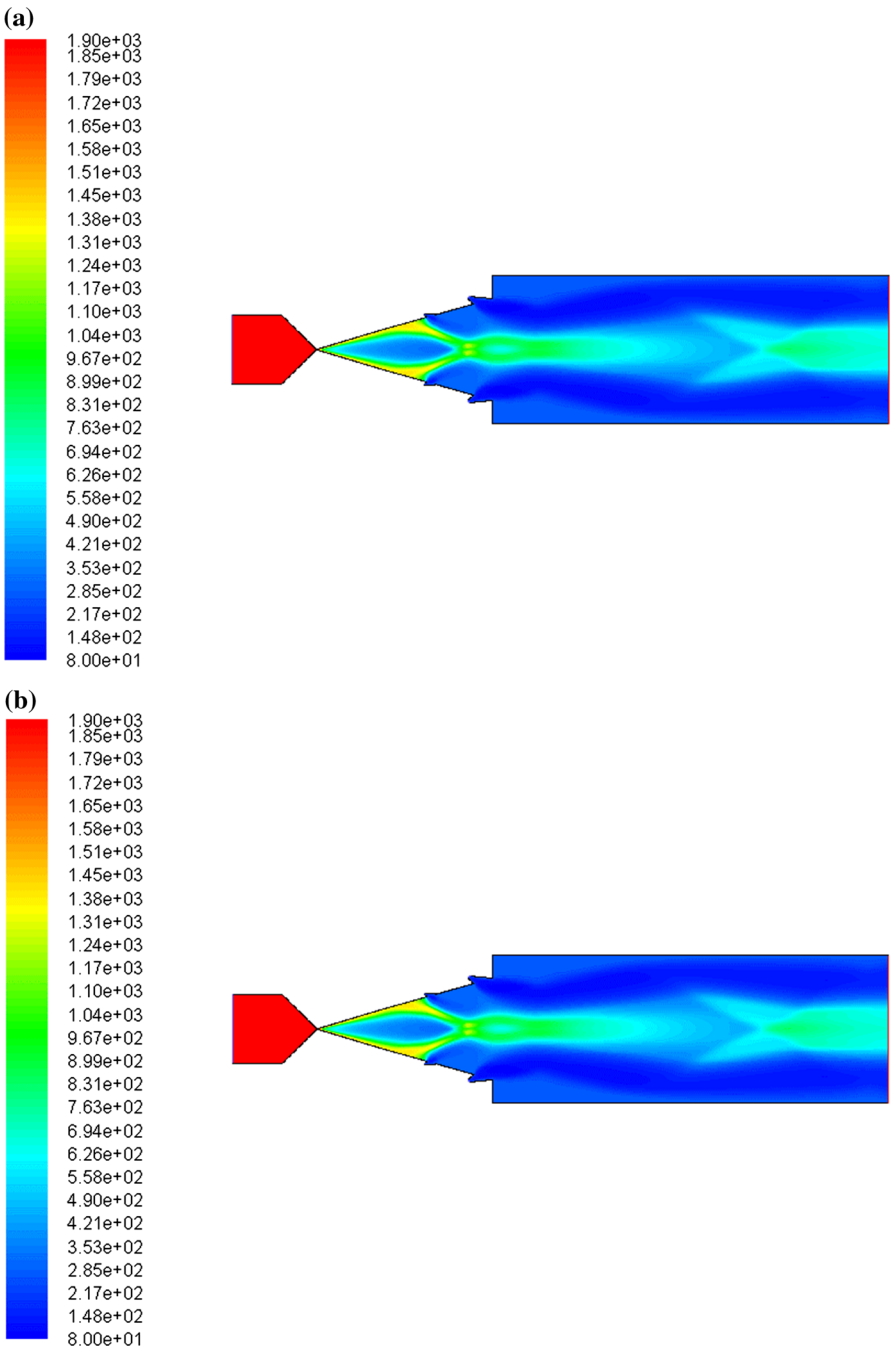

Fig. 4 Distribution of temperature. 16-species model (**a**) and 11-species model (**b**)

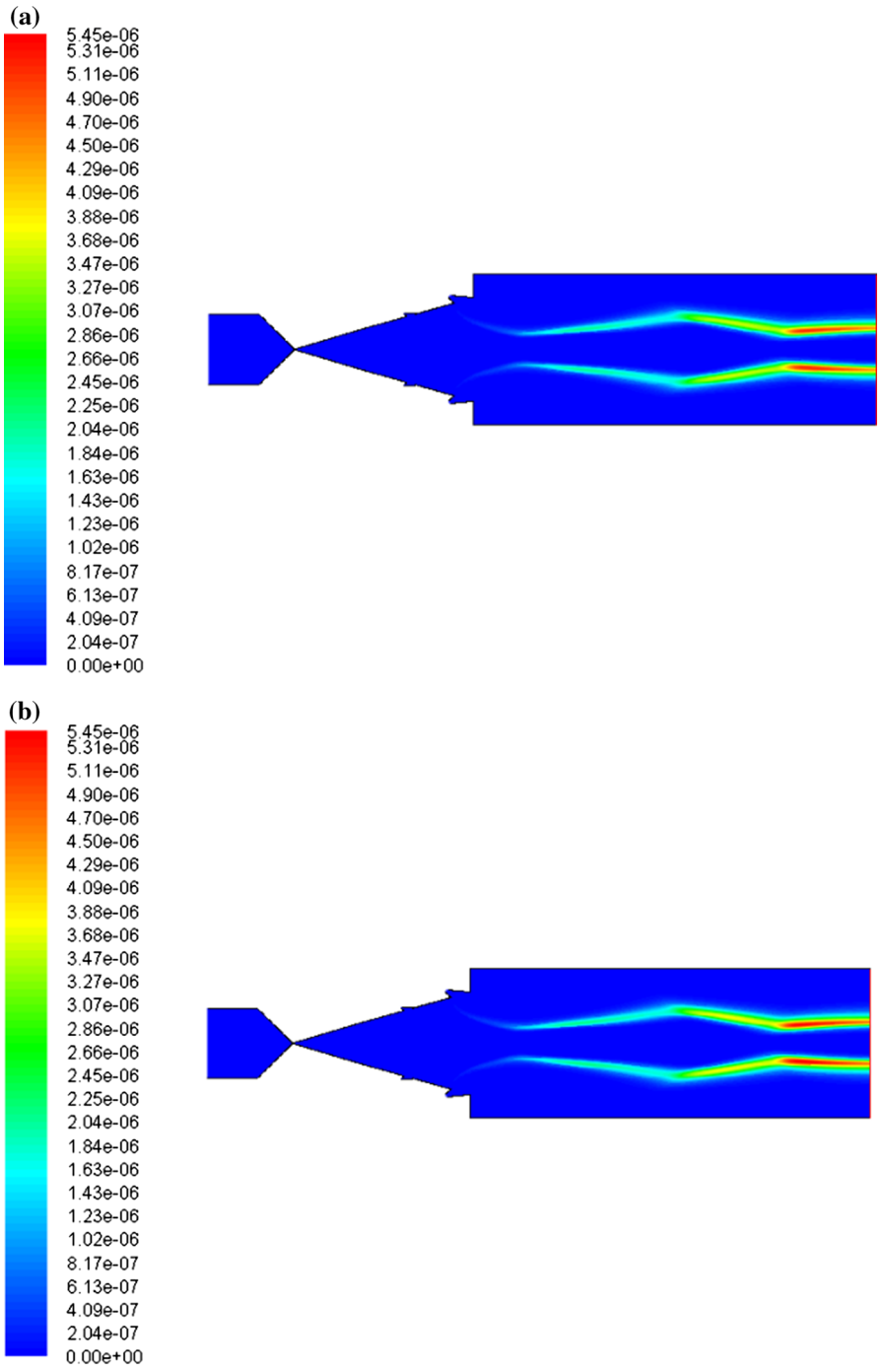

Fig. 5 Mole fraction of HF (2). 16-species model (**a**) and 11-species model (**b**)

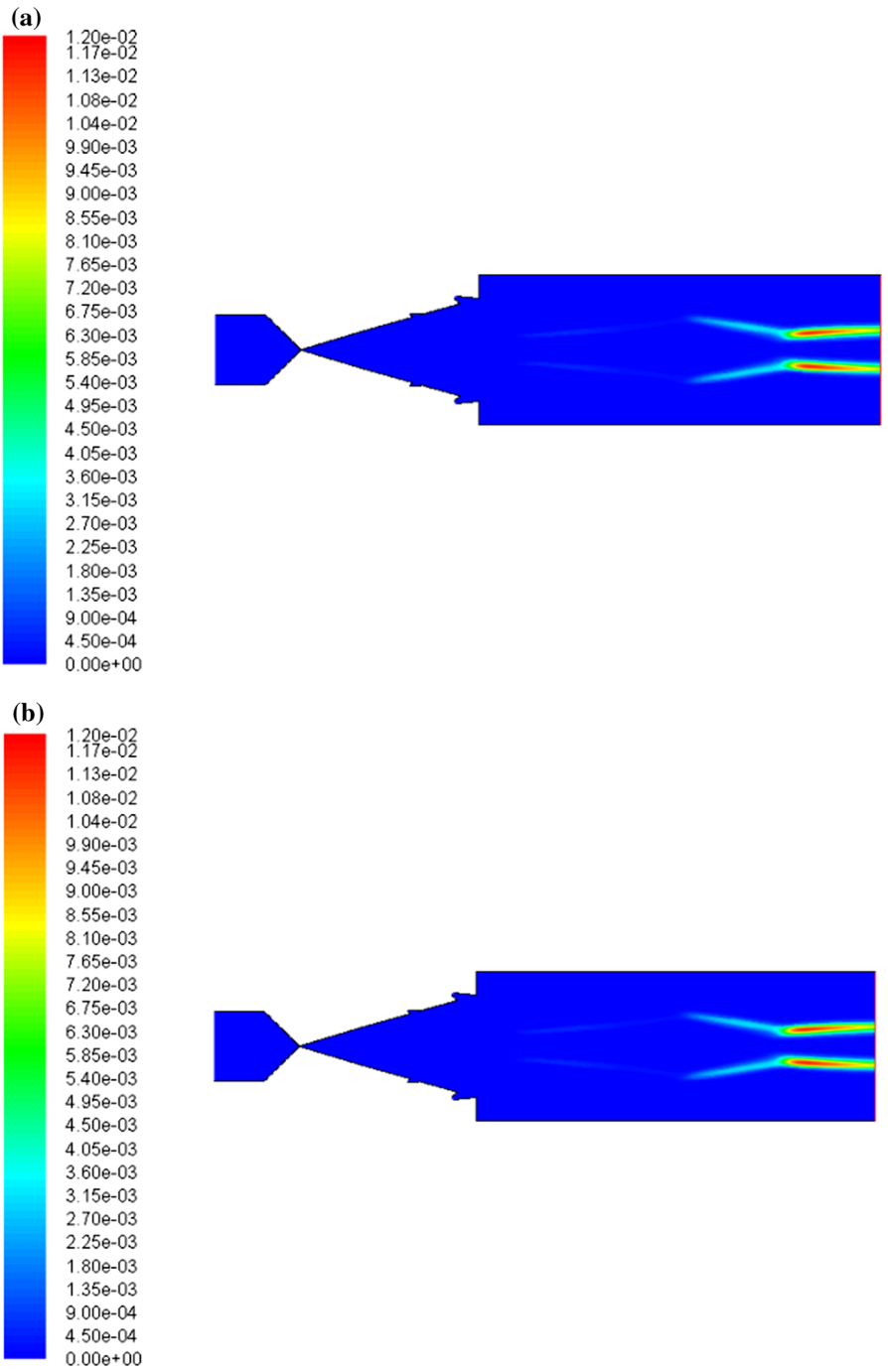

Fig. 6 Small signal gain of P_{11}. 16-species model (**a**) and 11-species model (**b**)

Figure 4 shows that the distribution of the gas flow in supersonic HF chemical laser. The temperature of the combustor is almost equal 1900 K, via the process of cooling by dilute gas in the secondary nozzle, and then mixed with H_2 in the cavity. The temperature distribution of the detailed mechanism and the reduced mechanism is almost same.

Figure 5 shows that mole fraction of HF (2) distribution. The distribution of HF (2) is at the bottom of optical cavity because of the speed of the injected of H_2 nozzle is low.

In this paper, the gain coefficient are calculated under the assumption of the equilibrium Boltzmann distribution for the rotational population at the translational temperature T. The rotational energy states for each vibrational state are given by

$$\rho_{\upsilon,J} = \rho_{\upsilon}\upsilon\frac{2J+1}{Q(\upsilon)}\exp\left(-\frac{\hbar c E_{\upsilon,J}}{k_B T}\right), \tag{15}$$

where $Q(\upsilon, J)$ is the rotational-partition function for a vibrational level, c is the speed of light, k_B is the Boltzmann constant, and $E_{\upsilon,J}$ is the rotational energy of state υ, J. Equations (14) and (15) are used to calculate the SSG, and the corresponding parameters are obtained from the paper [7]. Figure 6 shows the distribution of SSG. The distribution are in accordance with 16-species model and 11-species model.

From the above analysis, the reduced mechanism including 11 species and 39 reactions can describe the main feature of HF lasers. The low computational consuming model is important for numerical stimulation and experiments for design purpose.

6 Conclusions

In this paper, we developed a skeletal mechanism including 11 species and 58 elementary reactions for the HF chemical laser system. The results of skeletal mechanism with DRG, DRGSA, DRGEP and DRGEPSA are compared. The DRG and DRGSA methods have a significant drop, which shows that a stronger relation coupled among HF (4), HF (5) and HF (6). However, the DRGEP and DRGEPSA methods can orderly remove the species: HF (4), HF (7), HF (5) and HF (6). All these methods can provide an accurate skeletal mechanism with a rather small number of species. The DRG method is an effective tool to generate a skeletal mechanism with less time consuming and considerable accuracy in HF lasers. By using rate of production analysis, the skeletal mechanism is further reduced to 11 species and 39 elementary reactions.

To validate the reduced mechanism, this paper presents a numerical simulation of two-dimensional supersonic HF chemical lasers. The low computational consuming model can describe the main feature of HF lasers and is easy to implement for design purpose.

Acknowledgements This work was supported by the National Natural Science Foundation of China under Grant No. 21573218.

References

1. R. Gross, J. Bott, A.H. Reed, Handbook of chemical lasers. J. Electrochem. Soc. **124**, 235C–236C (1977)
2. G. Emanuel, Analytical model for a continuous chemical laser. JQSRT **11**, 1481–1520 (1971)
3. N. Cohen, A review of rate coefficients in the H2-F2 chemical laser system-supplement (1977), DTIC Document, 1978
4. N. Cohen, J.F. Bott, Review of rate data for reactions of interest in HF and DF lasers, DTIC Document, 1982
5. B.P. Aleksandrov, N.E. Vtorova, L.D. Isaeva, V.A.E. Shcheglov, Continuous-wave supersonic first-overtone chemical HF laser. Quantum Electron. **24**, 377 (1994)
6. M. Rotinian, M. Shur, M. Strelets, Navier–Stokes numerical simulation of supersonic hydrogen-fluorine combustion in CW chemical lasers. Symp. (Int.) Combust. **25**, 13–19 (1994)
7. G.C. Manke, G.D. Hager, A review of recent experiments and calculations relevant to the kinetics of the HF laser. J. Phys. Chem. Ref. Data **30**, 713–733 (2001)
8. B.P. Aleksandrov, A.A. Stepanov, Comparison of well-known kinetic models by the cw HF and DF chemical lasers numerical simulation—art. no. 67350A, in *International Conference on Lasers, Applications, and Technologies 2007: High-Power Lasers and Applications,* vol. 6735 (2007), pp. A7350
9. A.S. Boreysho, V.M. Malkov, A.V. Savin, High-power supersonic chemical lasers: gas-dynamic problems of operation of mobile systems with PRS, vol. 7131 (2008), p. 713103
10. T.F. Lu, C.K. Law, A directed relation graph method for mechanism reduction. Proc. Combust. Inst. **30**, 1333–1341 (2005)
11. P. Pepiot-Desjardins, H. Pitsch, An efficient error-propagation-based reduction method for large chemical kinetic mechanisms. Combust. Flame **154**, 67–81 (2008)
12. T.F. Lu, C.K. Law, On the applicability of directed relation graphs to the reduction of reaction mechanisms. Combust. Flame **146**, 472–483 (2006)
13. M. Valorani, F. Creta, D.A. Goussis, J.C. Lee, H.N. Najm, An automatic procedure for the simplification of chemical kinetic mechanisms based on CSP. Combust. Flame **146**, 29–51 (2006)
14. S.H. Lam, D.A. Goussis, The CSP method for simplifying kinetics. Int. J. Chem. Kinet. **26**, 461–486 (1994)
15. J.Y. Chen, A general procedure for constructing reduced reaction-mechanisms with given independent relations. Combust. Sci. Technol. **57**, 89–94 (1988)
16. T. Turanyi, Sensitivity analysis of complex kinetic systems—tools and applications. J. Math. Chem. **5**, 203–248 (1990)
17. A.E. Lutz, R.J. Kee, J.A. Miller, *SENKIN: A FORTRAN Program for Predicting Homogeneous Gas Phase Chemical Kinetics with Sensitivity Analysis* (Sandia National Labs, Livermore, 1988)
18. E. Horowitz, S. Sahni, S. Anderson-Freed, *Fundamentals of Data Structures* (Pitman, London, 1983)
19. C.F. Wisniewski, K.B. Hewett, G.C. Manke, C.R. Truman, G.D. Hager, Hydrogen fluoride overtone laser: 2D CFD modeling of the small signal gain, in *High-Power Laser Ablation,* vol. 5448, nos. 1 and 2 (2004), pp. 1127–1138